Vietnam Journal of Science and Technology ***61*** *(2) (2023) 246-254*

doi:10.15625/2525-2518/16615

The size-and shape-controlled synthesis of silver nanoparticles by solvothermal method

Nguyen Thi Ngoc Linh[1, *], Le The Tam[2], Ngo Thanh Dung[3], Le Thi Thanh Tam[3], Ha Minh Nguyet[3, 4], Nguyen Dinh Vinh[1], Bui Minh Quy[1], Nguyen Thi Hong Hoa[1], Nguyen Hoa Du[2], Nguyen Trung Thanh[5], Le Trong Lu[3, 4, *]

[1]*Thai Nguyen University of Sciences, Tan Thinh Ward, Thai Nguyen City, Viet Nam*

[2]*Vinh University, 182 Le Duan, Vinh City, Nghe An Province, Viet Nam*

[3]*Institute for Tropical Technology, Vietnam Academy of Science and Technology, 18 Hoang Quoc Viet, Ha Noi, Viet Nam*

[4]*Graduate University of Science and Technology, Vietnam Academy of Science and Technology, 18 Hoang Quoc Viet, Ha Noi, Viet Nam*

[5]*VNU University of Education, 144 Xuan Thuy, Cau Giay, Ha Noi, Viet Nam*

[*]Emails: *1. linhntn@tnus.edu.vn,2. tamlt@vinhuni.edu.vn, 3. ltlu@itt.vast.vn*

Received: 9 October 2021; Accepted for publication: 19 November 2021

Abstract. In this work, Ag nanoparticles (NPs) were fabricated by the solvothermal method of silver nitrate in different organic solvents with the presence of sodium oleate (SOA) and 1-octadecanol (OCD-ol). The effects of different solvents and concentrations of OCD-ol on the morphology and properties of the Ag nanomaterials were investigated in detail. The products were characterized by using transmission electron microscopy (TEM), X-ray diffraction (XRD), and absorption spectroscopy. The results showed that the type of solvents significantly affected the size and uniformity of the synthesized particles as well as the synthesis efficiency. Among three solvents, toluene, 1,2-dichlorobenzene (DCB), and tetralin, DCB with a moderate boiling point (181 ^{o}C) is the most appropriate solvent for synthesizing Ag nanoparticles. The concentration of the reductant OCD-ol clearly affects the morphology and size of Ag NPs. The concentration of 137.5 mM was proper for obtaining spherical and uniform Ag nanoparticles. The XRD analysis showed that the synthesized nanoparticles had good crystallinity. The surface plasmon resonance (SPR) properties of the Ag NPs was also dependent on the fabrication condition. The obtained Ag nanoparticles show potential applications in biomedicine, catalysis, or electronics.

Keywords: nanoparticles, Ag NPs, nanomaterials, solvothermal method, organic solvents.

Classification numbers: 2.2.1, 2.4.3.

1. INTRODUCTION

Ag NPs as the multifunctional nanomaterial have attracted the research interest of many scientists due to their remarkably physical, chemical, and biological characteristics such as

thermo-optic effect, electromagnetic properties, catalytic function, anti-bacterial and anti-fungi activities [1 - 3]. Previous studies showed that the application of Ag NPs relied on their size and shape. The spherical Ag NPs with a small size (< 15 nm) have been widely used in photothermia and antimicrobial therapies since they could take the advantage of small size for cell penetration [4]. The triangular Ag NPs have been applied extensively in analytical chemistry, pharmaceutical products, optical sensors, and catalysts [5 - 6]. Besides, Ag nanorods have been playing a significant role in many scientific fields owing to their high conductivity and excellent optical properties when compared to other forms in terms of surface plasmonic resonance. In practice, Ag nanorods are used in optoelectronic devices and electromagnetic field generators in field-emission displays [7].

Generally, Ag NPs can be fabricated by using physical, biological, and chemical methods [8 - 10] in which the chemical method is relatively low-cost and does not require expensive specialized devices. In this method, Ag NPs can be fabricated in the aqueous or organic media. The reported study showed that the synthesis of Ag NPs in the aqueous environment still faced the limitation such as difficulty in controlling the size and shapes [11] while the synthesis in organic solvents has exhibited the effectiveness in tuning the size, dispersion and uniformity of the NPs [12]. However, the control of morphology and size of Ag NPs in organic solvent has not been studied systematically yet. In this work, we synthesized Ag NPs in different solvents at their boiling points, using 1-octadecanol as reductant and sodium oleate as an intermediate complexing agent and simultaneously surfactant. By changing reaction conditions (organic solvent and reductant concentration), the shape of Ag NPs could be varied from spherical to triangular, cubic, and rod shapes with diverse sizes. The morphology and surface plasmon resonance property of Ag NPs were also tuned through reaction conditions.

2. EXPERIMENTAL

2.1. Chemicals

The chemicals used for the synthesis of Ag NPs were analytical grade and ordered from Sigma Aldrich company with purity ≥ 99 %, including silver nitrate ($AgNO_3$), sodium oleate (SOA), 1-octadecanol (OCD-ol), toluene, 1,2-dichlorobenzene (DCB), 1,2,3,4-tetrahydronaphthalene (tetralin), ethanol and *n*-hexane.

2.2. Synthesis of Ag NPs

The Ag NPs were synthesized by the solvothermal method in organic solvents at the boiling point of the solvents. In detail, a mixture containing 1 g of $AgNO_3$, 2 g of SOA, and 40 mL of organic solvent (toluene, DCB or tetralin) was magnetically stirred under nitrogen flow in 30 min at room temperature. The reductant OCD-ol with a concentration range of 92.5 - 370 mM was added to the reaction mixture. The reaction system was then refluxed at the boiling point of the corresponding solvent for 90 min.

The as-synthesized Ag NPs were collected and washed as follows: An amount of sample solution was well-mixed with ethanol and then centrifuged at 10 000 - 12 000 rpm for 10 min. After discarding the solvent, the particles were re-dispersed into *n*-hexane and precipitated by ethanol. The washing process was repeated five times. The obtained Ag NPs were re-dispersed into *n*-hexane.

2.3. Characterization methods of Ag NPs

The morphology of Ag NPs was determined by Transmission Electron Microscopy (TEM) using JEM 1010 (Japan). The crystalline phase analysis was carried out on an X-ray diffractometer – SIEMENS D5005 using radiant Cu K_α (λ = 1.5406 Å). The UV-Vis spectra of the samples were recorded on a Jasco V-670 spectrometer (Japan).

3. RESULTS AND DISCUSSION

3.1. Influence of solvents on the morphology and optical properties of the Ag NPs

The morphology of Ag NPs can be controlled by seed formation and growth stages. This process is strongly influenced by parameters such as concentration of reactants, type of solvents, reaction temperature, etc. [13]. Figure 1 shows the effect of some solvents (toluene, DCB, tetralin) on the morphology, size, and synthesis efficiency of the as-synthesized Ag NPs.

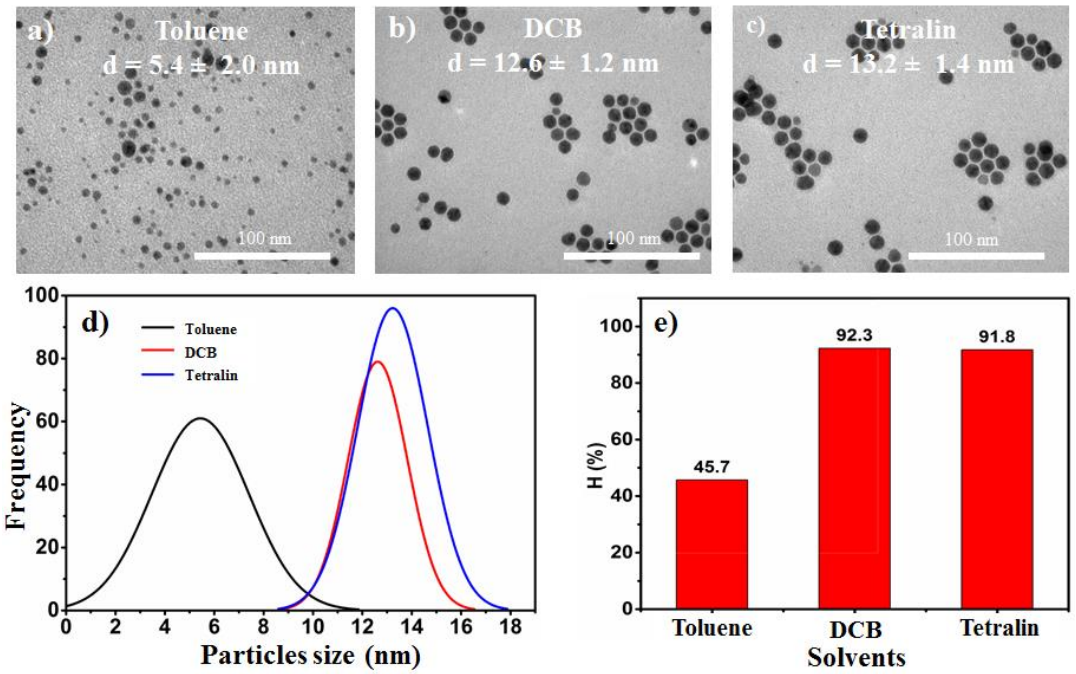

Figure 1. TEM images (a-c), size distribution chart (d) and the synthesis efficiency (e) of the Ag NPs in different solvents.

From Figure 1, the shape and size of Ag NPs are affected by the type of solvents used in the synthesis procedure. The Ag NPs fabricated in toluene solvent at 110 ^oC (boiling point of toluene) are spherical but non-uniform with an average size of 5.4 ± 2.0 nm and a high stdev (standard deviation) of 37 % (Figure 1a). For DCB solvent with a boiling point of 181 ^oC, the obtained particles have a relatively uniform spherical shape with a clear border, an average size of 12.6 ± 1.2 nm, and the stdev in this case is quite small (9.5 %) (Figure 1b). The NPs obtained in tetralin solvent at 208 ^oC (boiling point of the solvent), the NPs are uniform and spherical with an average size of 13.2 ± 1.4 nm, and the stdev of 10.6 % (Figure 1c). Hence, it can be concluded that using solvent at the higher boiling point can create Ag NPs with a larger average

size (Figure 1d) and a higher synthesis efficiency (Figure 1e). This observation can be explained that in toluene solvent with a lower boiling point (110 ^{o}C), the reaction is slow and incomplete, leading to the non-uniformity of Ag NPs, the wideness of the size distribution, and the low synthesis efficiency (45.7 %). For DCB and tetralin solvents, the higher temperature (181 and 208 ^{o}C) accelerates the seed formation and growth, resulting in the homogeneity of the Ag NPs and the high synthesis efficiency (> 90 %) due to the completion of the reaction. Accordingly, the type of solvents is an important factor affecting the size and uniformity of the synthesized particles as well as the synthesis efficiency. Among investigated solvents, DCB with a moderate boiling point (181 ^{o}C) is the most appropriate solvent due to high uniformity, the small stdev (9.5 %), and high efficiency (92.3 %), thus this solvent was chosen for further investigation.

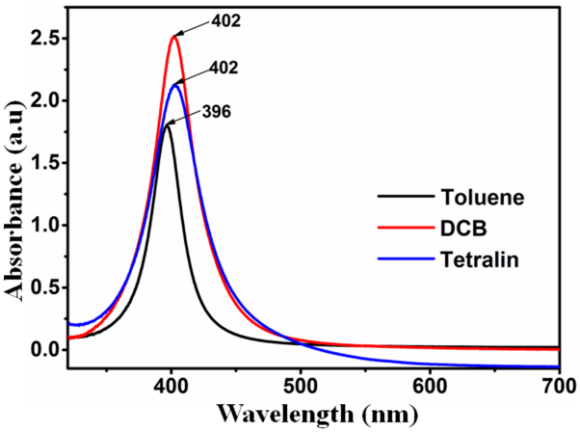

Figure 2. UV-vis spectra of Ag NPs synthesized in different solvents.

The optical properties of Ag NPs were studied by UV-Vis spectroscopy and the results are presented in Figure 2. In all three spectra, there is a clear surface plasmonic resonance (SPR) range with high absorption intensity corresponding to the characteristic peaks of Ag NPs. When the particle size increased from 5.4 to 13.2 nm, these SPR peaks shifted from 396 to 402 nm. Obviously, the position and shape of the SPR ranges of Ag NPs are governed by the size and shape of the fabricated particles in different solvents. According to the Mie theory [14], there is only one SPR peak in the absorption spectrum of the spherical particles, while anisotropic particles can generate two or more SPR peaks depending on their shapes. In Figure 2, only one SPR peak can be observed, indicating that the Ag NPs have a spherical shape. This result is also proved by TEM images (Figure 1).

3.2. Influence of reductant concentration on morphology and optical properties of Ag NPs

During the formation of Ag NPs, sodium oleate (SOA) acts as the intermediate complexing agent with Ag^{+} and surfactant preventing the agglomeration of particles, while OCD-ol functions as the reductant (reducing Ag^{+} to form Ag). To further understand the influence of OCD-ol concentration on the morphology and properties of Ag NPs, the OCD-ol concentration was varied from 92.5 to 370 mM. All samples were synthesized in DCB solvent at 181 ^{o}C. The morphology of material was studied by TEM and the results are presented in Figure 3 and Table 1.

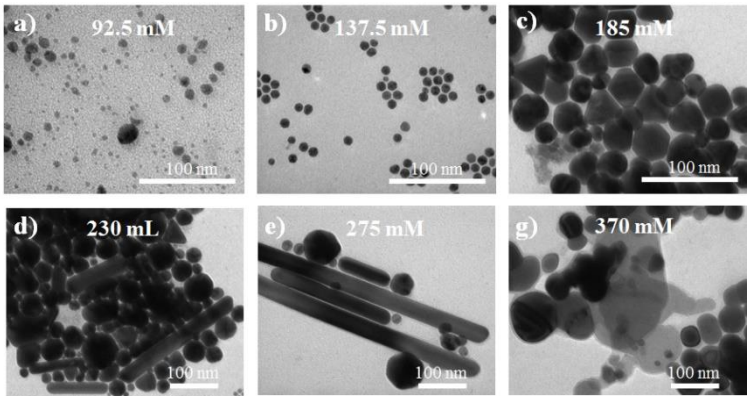

Figure 3. TEM images of Ag NPs at different concentrations of the reductant OCD-ol.

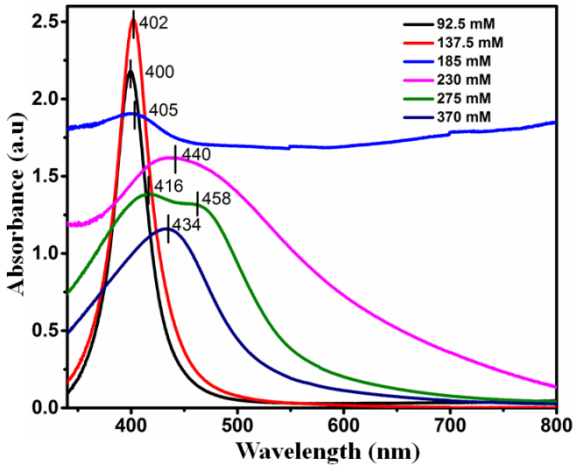

Figure. 4. UV-Vis spectra of Ag NPs synthesized at different concentrations of the reductant OCD-ol.

As presented in Figure 3a, the concentration of the reductant OCD-ol clearly affects the morphology and size of Ag NPs. The sample prepared in OCD-ol at the concentration of 92.5 mM contains non-uniform spherical particles with an average size of 7.8 ± 2.6 nm and a high value of the small stdev (33.3 %). When the concentration increases to 137.5 mM, the obtained spherical Ag NPs are more uniform with an average size of 12.6 ± 1.2 nm and the stdev of 9.5% (Figure 3b). The Ag NPs obtained with the OCD-ol concentration of 185 mM have various shapes such as spheres, triangles, and cubes with large average size of 48.7 ± 3.4 nm. In the sample with OCD-ol concentration of 230 mM, besides nanospheres, nano triangles, and nanocubes, a small amount (approximately 4 %) of Ag nanorods with an average diameter of 30.2 nm and lengths ranging from 100 to 220 nm can be observed. At OCD-ol concentration of 275 M, only a small amount of Ag nanospheres formed while the product mainly contains Ag nanorods with an average diameter of 32.5 nm and diverse lengths. When the concentration increases to 370 mM, Ag nanospheres agglomerated with a large average size of 78.6 ± 7.3 nm can be observed. Thus, the size and shape of Ag NPs significantly depend on the concentration of OCD-ol. Data of particles size can be explained by the classical nucleation/diffusion growth model [15]. Herein, Ag^0 atoms initially formed can gather and create seeds to form a certain quantity of particles at the early stage of reaction and the Ag NPs formed later can deposit on the present particles. When the OCD-ol concentration of 92.5 mM is not enough to completely

reduce Ag^+ ions, the Ag^+ reduction rate is slow then a small amount of Ag is formed. At the concentration of 137.5 mM, the reduction rate increases, facilitating the growth of Ag NPs with uniform size. The non-uniformity in size of the sample with the reductant concentration of 92.5 mM is caused by the lower concentration of Ag^0 seed crystals compared to that in a solution containing 137.5 mM, whilst the critical size becomes larger. On the other hand, based on the theory of the growth process of seed crystals, low concentration of monomers and low reaction rate of precursors during synthesis lead to Ostwald ripening process [16]. That explains the wide size distribution of Ag NPs at low concentrations of OCD-ol. When the reductant concentration increases to 185 mM, the Ag seeds continuously form and ripen to Ag nanoparticles with different shapes (spheres, triangles, cubes) and larger sizes. This may be caused by the selective adsorption of the newly formed Ag atoms on the surface of the previously formed seed crystals. As the reductant concentration is 230 mM and 275 mM, the reduction rate of Ag^+ continues to rise and the amount of Ag atoms increases, then Ag particles transform to Ag rods. However, huge quantity of Ag^0 seeds formed at OCD-ol concentration of 370 facilely agglomerate into nano globe. The results indicate that the different reduction rates of OCD-ol play a crucial role in controlling the morphology of Ag nanomaterials from nanosphere to nanorod.

Effects of OCD-ol concentrations on optical properties of materials were also studied by UV-Vis spectroscopy and results are demonstrated in Figure 4 and Table 1. Clearly, the samples synthesized at concentrations of 92.5 and 137.5 mM have only one SPR peak at 400 and 402 nm, respectively, with a relatively narrow half-width of plasmonic peak characterizing for Ag element. For the samples prepared at 185 and 230 mM of OCD-ol, there is a maximum absorption at the wavelength of 405 and 440 nm, respectively, with a significantly broad SPR peak compared to those of the samples prepared at 92.5 mM and 137.5 mM. These results can be explained by the increase in the size and the change in morphology of Ag NPs. As the size of Ag NPs becomes larger, the SPR peak broaden and strongly shift toward the longer wavelength range (redshift). When the concentration of OCD-ol of 275 mM, the UV-Vis spectra show two SPR peaks at 416 and 458 nm due to the formation of Ag nanorods. However, if the concentration of OCD-ol is 370 mM, the UV-Vis spectrum has only one SPR peak at the position of 434 nm because of the formation of the giant agglomerated Ag globes. Therefore, the position and shape of SPR ranges of Ag nanomaterials are governed by the size and shape of the particles. This conclusion is totally in agreement with Mie theory [14].

Table 1. Effect of OCD-ol concentrations on morphology and optical properties of Ag NPs.

Concentrations of OCD-ol (mM)	Morphology	SPR (nm)
92.5	Spheres	400
137.5	Spheres	402
185	Spheres, triangles and cubes	405
230	Spheres, triangles, cubes, and rods	440
275	Spheres, and rods	416 and 458
370	Spheres	434

3.3. Crystalline phase of Ag NPs

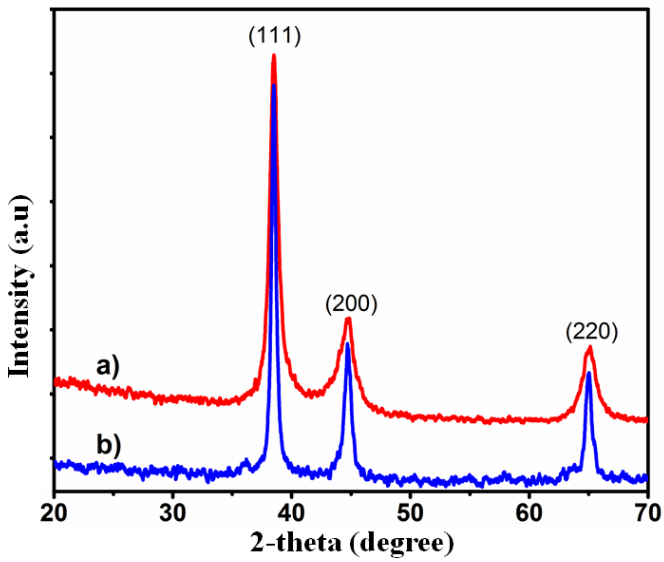

Figure. 5. Xray diffraction patterns of the spherical Ag NPs (a) and Ag nanorods (b).

To evaluate the crystallinity of Ag NPs, we conducted X-ray diffraction analysis on some representative samples among the synthesized materials. Figure 5 illustrates the X-ray diffraction patterns of spherical (137.5 mM of OCD-ol) and rod (275 mM of OCD-ol) Ag NPs. The patterns show that the products only contain Ag NPs with high purity and a face-centered cubic structure (fcc). Both samples have characteristic peaks at $2\theta = 38.0^{o}$; 44.2^{o} and 64.21^{0} corresponding to the crystal planes (111), (200) and (220) characterizing for Ag crystals (JCPDS, 004-0783).

4. CONCLUSIONS

The Ag NPs with various morphologies have been successfully synthesized by the solvothermal method. The reaction parameters including types of solvents and the reductant OCD-ol concentrations influenced the shape, size, uniformity, and optical properties of Ag NPs. On large-scale fabrication, the facile approach can easily tune the shape and size of materials, opening great application potential of Ag NPs in biomedicine, catalysis, and electronics fields.

Acknowledgement. This research is funded by the Thai Nguyen University of Sciences under grant number CS2021-TN06-17.

CRediT authorship contribution statement. Le The Tam, Ngo Thanh Dung, Le Thi Thanh Tam: synthesis of materials; Ha Minh Nguyet, Nguyen Dinh Vinh: performed measurements (XRD, TEM, UV-Vis); Bui Minh Quy, Nguyen Thi Hong Hoa: performed analysis and assessment of morphology and structure; Nguyen Hoa Du: Writing – original draft; Nguyen Thi Ngoc Linh, Le Trong Lu: Supervision, Writing – review & editing. All authors read and approved the final manuscript.

Declaration of competing interest. There are no conflicts to declare.

REFERENCES

1. D'Agostino A., Taglietti A., Desando R., Bini M., Patrini M., Dacarro G., Cucca L., Pallavicini P., and Grisoli P. - Bulk surfaces coated with triangular silver nanoplates: Antibacterial action based on silver release and photo-thermal effect, Nanomaterials **7** (1) (2017) 7-22. doi:10.3390/nano7010007.
2. Abdel-Fattah W. I. and Ali G. W. - On the anti-cancer activities of silver nanoparticles, J. Appl. Biotechnol. Bioeng. **5** (1) (2018) 43-46. doi: 10.15406/jabb.2018.05.00116.
3. Konopatsky A. S., Leybo D. V., Firestein K. L., Popov Z. I., Bondarev A. V., Manakhov A. M., Permyakova E. S., Shtansky D. V., and Golberg D. V. - Synthetic routes, structure and catalytic activity of Ag/BN nanoparticle hybrids toward CO oxidation reaction, J. Catal. **368** (2018) 217-227. doi: 10.1016/j.jcat.2018.10.016.
4. Siritongsuk P., Hongsing N., Thammawithan S., Daduang S., Klaynongsruang S., Tuanyok A., Patramanon R. - Two-phase bactericidal mechanism of silver nanoparticles against Burkholderia Pseudomallei, PLoS One **11** (12) (2016) 0168098-0168119. doi: 10.1371/journal.pone.
5. Zhong Y., Liang G., Jin W., Jian Z., Wu Z., Chen Q., Cai Y., and Zhang W. - Preparation of triangular silver nanoplates by silver seeds capped with citrate-CTA^+, RSC Adv. **8** (51) (2018) 28934-28943. doi: 10.1039/c8ra04554b.
6. Furletov A. A., Apyari V. V., Garshev A. V., Dmitrienko S. G., and Zolotov Y. A. - Triangular silver nanoplates as a spectrophotometric reagent for the determination of mercury(II), J. Anal. Chem. **72** (12) (2017) 1203-1207. doi:10.1134/S1061934817120061.
7. Shalaby M. S., Abdallah H., Chetty R., Kumar M. and Shaban A. M. - Silver nano-rods: Simple synthesis and optimization by experimental design methodology, Nano-Structures and Nano-Objects **19** (2019) 100342-100351. doi: 10.1016/j.nanoso.2019.100342.
8. Li Y., Kim Y. N., Lee E. J., Cai W. P., and Cho S. O. - Synthesis of silver nanoparticles by electron irradiation of silver acetate, Nucl. Instruments Methods Phys. Res. B **251** (2) (2006) 425-428. doi:10.1016/j.nimb.2006.06.019.
9. Arya A., Gupta K., Chundawat T. S., and Vaya D. - Biogenic synthesis of copper and silver nanoparticles using green alga botryococcus braunii and its antimicrobial activity, Bioinorg. Chem. Appl. **2018** (2018) 1-9. doi: 10.1155/2018/7879403.
10. Purna G., Rao C., and Yang J. - Chemical reduction method for preparation of silver nanoparticles on a silver chloride substrate for application in surface-enhanced infrared optical sensors, Appl. Spectrosc. **64** (10) (2010) 1094-1099. doi:10.1366/ 000370210792973640.
11. Salvioni L., Galbiati E., Collico V., Alessio G., Avvakumova S., Corsi F., Tortora P., Prosperi D., and Colombo M. - Negatively charged silver nanoparticles with potent antibacterial activity and reduced toxicity for pharmaceutical preparations, Int. J. Nanomedicine **12** (2017) 2517-2530. doi: 10.2147/IJN.S127799.
12. Hiramatsu H. and Osterloh F. E. - A simple large-scale synthesis of nearly monodisperse gold and silver nanoparticles with adjustable sizes and with exchangeable surfactants, Chem. Mater. **16** (13) (2004) 2509-2511. doi: 10.1021/cm049532v.
13. Thanh N. T. K., Maclean A. N., and Mahiddine S. - Mechanisms of nucleation and growth of nanoparticles in solution, Chem. Rev. **114** (15) (2014) 7610-7630. doi:

10.1021/cr400544s.

14. Mayer K. M. and Hafner J. H. - Localized surface plasmon resonance sensors, Chem. Rev., **111** (2011) 3828-3857. doi: 10.1021/cr100313v.
15. LaMer V. K., Dinegar R. H. - Theory, production and mechanism of formation of monodispersed hydrosols, J. Am. Chem. Soc. **72** (11) (1950) 4847-4854. doi: 10.1021/ja01167a001.
16. Yin Y. and Alivisatos A. P. - Colloidal nanocrystal synthesis and the organic-inorganic interface, Nature **437** (7059) (2005) 664-670. doi:10.1038/nature04165.